Immunity, Volume *38*

Supplemental Information

Maturation of Lymph Node Fibroblastic Reticular Cells from Myofibroblastic Precursors Is Critical for Antiviral Immunity

Qian Chai, Lucas Onder, Elke Scandella, Cristina Gil-Cruz, Christian Perez-Shibayama, Jovana Cupovic, Renzo Danuser, Tim Sparwasser, Sanjiv A. Luther, Volker Thiel, Thomas Rülicke, Jens V. Stein, Thomas Hehlgans, and Burkhard Ludewig

Supplemental Inventory

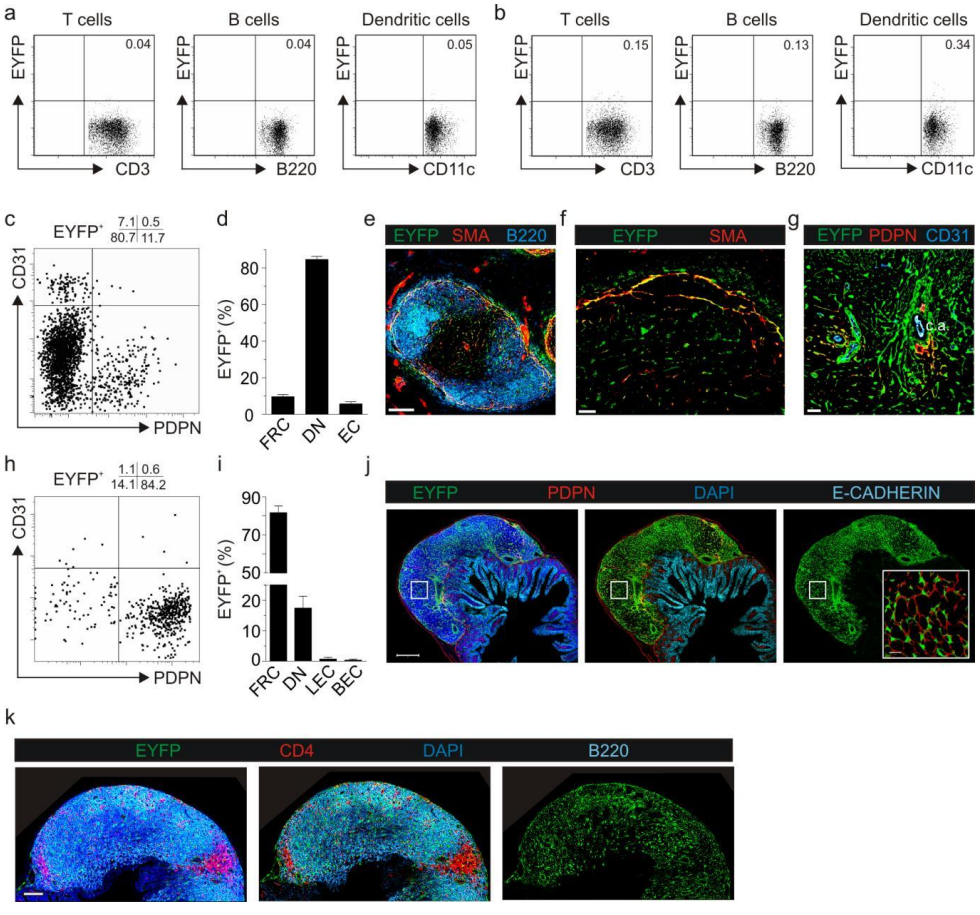

Figure S1. Transgene Expression in Secondary Lymphoid Organs of *Ccl19-cre* Mice, Related to Figure 1

(a-b) Lack of *Ccl19-cre* transgene activity in non-stromal LN cells. LN cell suspensions from 6 wk old *Ccl19-crexR26-eyfp* (a) or *Ccl19-cre* control mice (b) were stained with antibodies against CD45, CD3, B220, and CD11c. EYFP expression in the different CD45+ cell populations was determined by flow cytometry. Values in the upper right quadrant of one representative dot plot analyses out of six indicate EYFP-positive cells in the respective cell population.

(c-g) *Ccl19-cre* expression in splenic stromal cells. (c) Spleen cell suspensions from 6 wk old *Ccl19-crexR26-eyfp* mice were depleted of CD45+ cells, and EYFP expression was determined by flow cytometry. Representative dot plot analysis with percentage of EYFP expression in CD45– splenic stromal cells. (d) EYFP expression in CD45– splenic stromal cell populations (PDPN+CD31– fibroblastic reticular cells (FRC); PDPN–CD31– double negative cells (DN); CD31+ endothelial cells (ECs)); mean percentage±SEM (n=6 mice). (e) Confocal microscopic analysis of splenic white pulp *Ccl19-crexR26-eyfp* section using antibodies against the indicated markers, scale bar = 100 μm. High resolution analysis of EYFP expression in splenic marginal zone (f) and central arteriole area (c.a.) (g).
(h-k) *Ccl19-cre* expression in Peyer's patch (PP) stromal cells.

(h) PP single cell suspensions from 6 wk old *Ccl19-crexR26-eyfp* mice were depleted of CD45+ cells, and EYFP expression was determined by flow cytometry. Representative dot plot analysis with percentage of EYFP expression in CD45– PP stromal cells.

(i) EYFP expression in CD45– PP stromal cell populations (PDPN+CD31– fibroblastic reticular cells (FRC); PDPN–CD31– double negative cells (DN); PDPN–CD31+ blood endothelial cells (BEC); PDPN+CD31+ lymphatic endothelial cells (LEC)); mean percentage±SEM (n=4 mice).

(j, k) Confocal microscopic analysis of PP in *Ccl19-crexR26-eyfp* mice using antibodies against the indicated markers, scale bar in (j) = 200 μm, scale bar in (k) = 50 μm.

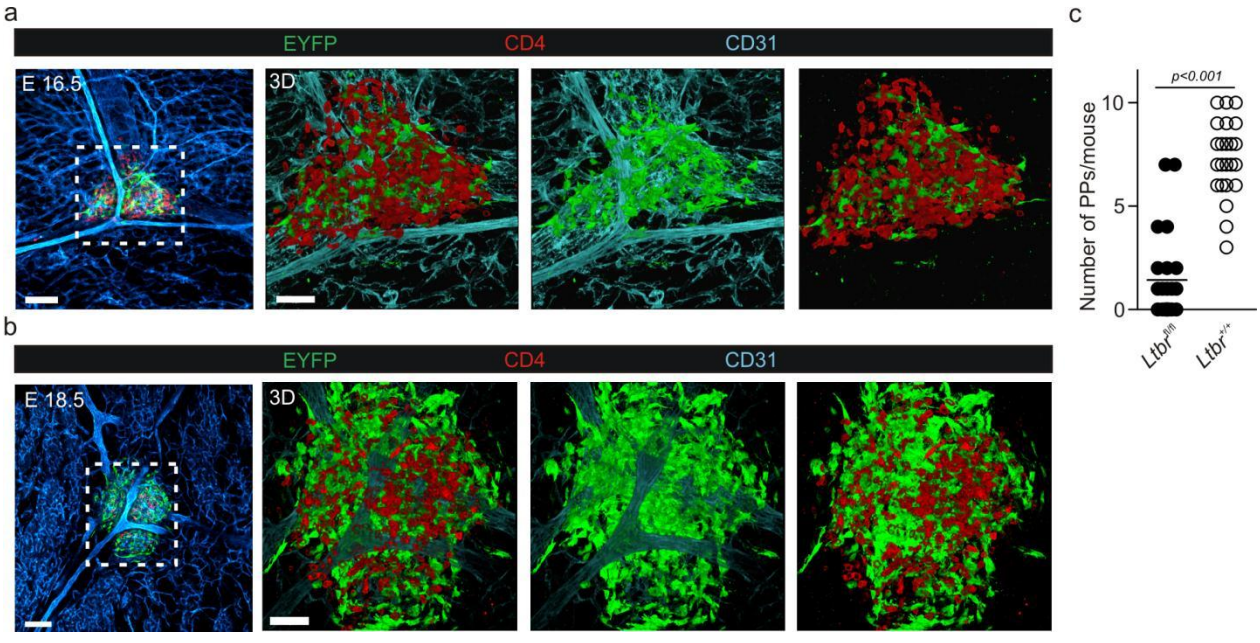

Figure S2. LN and PP Development in *Ccl19-cre* Mice, Related to Figure 2

(a-b) Characterization of *Ccl19-cre*+ mesenchymal stromal cells in developing LNs at embryonic days (E) 16.5 (a) and E18.5 (b). *Ccl19-cre*x*R26-eyfp* embryos were analyzed for transgene expressing cells (EYFP+, green) in inguinal LN anlagen by confocal microscopy. The characteristic branching pattern of the blood vessels (CD31+, blue) and accumulation of LTi cells (CD4+, red) facilitated localization of the anlage (left panels in (a) and (b)); scale bars = 40 μm. Right panels show 3D reconstructions of the boxed area in left panel, scale bars = 100 μm. Representative data from one out of three samples per time point.

(c) Presence of PPs in 6 wk old *Ccl19-cre*x*Ltbr*fl/fl and *Ltbr*+/+ mice was assessed following Evan's Blue application. Values indicate number of detectable PPs per mouse in the indicated strain.

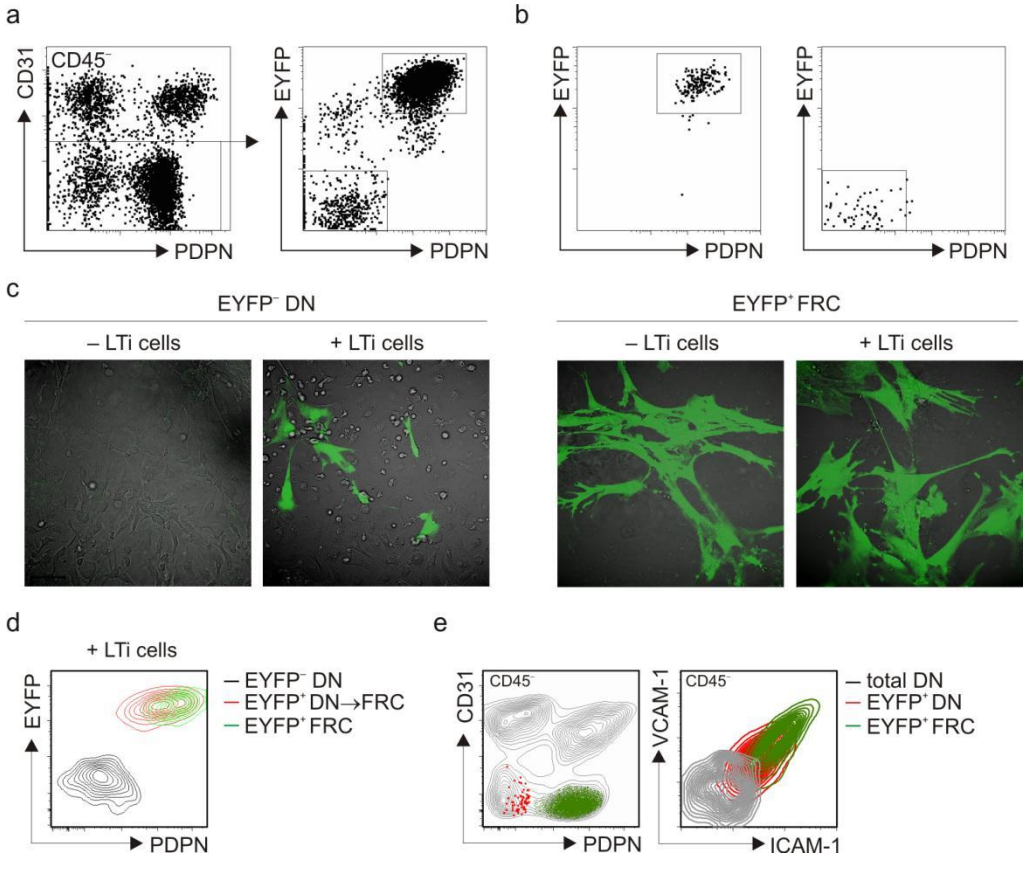

Figure S3. Maturation of *Ccl19-cre*-Expressing Stromal Cells, Related to Figure 5

(a) CD31– LN stromal cells from *Ccl19-crexR26-eyfp* mice were sorted by flow cytometry into PDPN–EYFP– double-negative (DN) and PDPN+EYFP+ FRCs (n=6 mice).

(b) Post-sorting confirmation of cell purity. (c) EYFP– DN cells and EYFP+ FRCs were cultured in vitro on basement membrane protein-coated plates in the absence or presence of B220–CD3–CD11c–CD3–CD4+ LTi cells obtained from spleens of recombination-activating gene (RAG)-deficient mice. Seven days later, EYFP expression was determined by confocal laser scanning microscopy. Microphotographs show representative areas of stromal cell cultures in an overlay of phase-contrast light microscopy and immunofluorescence.

(d) Flow cytometric analysis of PDPN expression on the indicated stromal cell populations following in vitro co-cultivation with LTi cells.

(e) Flow cytometric analysis showing representative contour plot of CD31- and PDPN-expressing, pooled CD45– LTβR-competent LN stromal cells (left panel) with back-gating of ICAM1- and VCAM1-expressing cell populations as indicated in the right panel. Representative data from one out of two independent experiments.

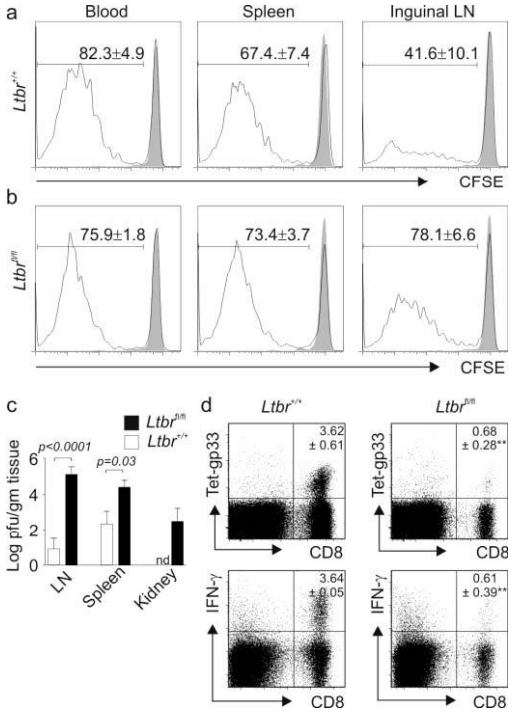

Figure S4. Immune Reactivity in the Absence of LTβR-Mediated FRC Maturation, Related to Figure 6

(a-b) Dendritic cell (DC)-T cell interaction in the absence of LTβR-mediated FRC maturation. Two million CFSE-labeled CD8+ T cells expressing a T cell receptor specific for the MHV spike protein-derived, H2-Kb-binding S598 epitope (TCR-S) were adoptively transferred into *Ltbr*+/+ (a) or *Ccl19-crexLtbr*fl/fl mice (b) using intravenous injection. One day later, recipients were immunized subcutaneously into the right flank with 2.5×105 bone marrow-derived DCs pulsed with S598 peptide. T cell activation was determined on day 3.5 post DC immunization in blood, spleen and skin-draining inguinal LN by flow cytometry (black lines). Control mice received CSFE-labeled TCR-S cells i.v. and 2.5×105 bone marrow-derived DCs s.c. with peptide (grey-shaded histograms). Values in histograms indicate mean percentage±SEM of proliferated cells pooled from 2 independent experiments (n= 4 mice).

(c-d) Assessment of immune reactivity against LCMV infection in the absence of FRC-specific LTβR signaling. *Ccl19-crexLtbr*fl/fl and *Ltbr*+/+ mice were infected intravenously with 200 pfu of LCMV WE. (c) Viral titers in the indicated organs were determined at day 8 post infection (mean viral titers±SEM, n=7 mice); nd, not detectable. (d) Antiviral CD8+ T cell responses in LNs were determined by H2-Db-gp33 tetramer analysis (upper panels) and intracellular staining for gp33-responsive IFN-γ-producing CD8+ T cells (lower panels). Values in the upper right quadrant indicate mean percentages±SEM of specific cells in the lymphocyte gate, n=6 mice (**, $p<0.01$).